Spring 2013

Robust methods for construction of global potential energy surfaces

Phalgun Lolur

ROBUST METHODS FOR CONSTRUCTION OF GLOBAL POTENTIAL

ENERGY SURFACES

by

PHALGUN LOLUR

A THESIS

Presented to the Faculty of the Graduate School of the

MISSOURI UNIVERSITY OF SCIENCE AND TECHNOLOGY

In Partial Fulfillment of the Requirements for the Degree

MASTER OF SCIENCE IN CHEMICAL ENGINEERING

2013

Approved by

Daniel Forciniti, Advisor
Richard Dawes, Co-Advisor
Jee-Ching Wang

ABSTRACT

This thesis is about the development of robust methods for construction of global potential energy surfaces to study the spectroscopy and dynamics of molecular systems. A potential energy surface represents the electronic energy of a molecule as a function of its geometry. This is central to how chemists view molecular systems in terms of motion across a rich energy landscape where barriers separate wells corresponding to different stable structures. The range of molecular distortions defines the potential energy surface. Computing the potential energy surface of a molecule has become a fundamental operation in modern theoretical chemistry studies. The Born–Oppenheimer approximation simplifies the Schrödinger equation (since the nuclei move slowly relative to the electrons), and enables computation of energies forming the surface. In order to develop a highly accurate surface, it is generally required to compute energies at many (typically thousands) molecular geometries. These data are then fit together using an interpolative scheme to form an analytic function.

Due to interaction between states, in order to develop a surface for a particular state of interest, one often needs to include several states. In a multistate calculation, states are optimized for some choice of relative weights. It is necessary to dynamically adjust the weights, as the geometry is varied, in order to obtain a smooth and continuous surface (as using fixed weights can lead to disruptive discontinuities where states switch character). This project developed a weighting scheme based on an energy dependent functional designed to produce high accuracy and robust convergence for global surfaces. This method has been successfully demonstrated on ozone. The theoretical calculations are in good agreement with experiments, producing a significant improvement of the rate constant for the $O + O_2$ exchange reaction.

ACKNOWLEDGMENTS

TABLE OF CONTENTS

LIST OF ILLUSTRATIONS

LIST OF TABLES

1. INTRODUCTION

By the end of the nineteenth century, many scientists believed that most of the fundamental laws and equations had already been worked out. The only improvements that they expected were minor refinements in the theories to get that extra decimal place of accuracy in their calculations. But everything changed when quantum mechanics came into the picture in the early twentieth century. Max Planck, who is considered as the father of the quantum theory, came up with his hypothesis (which was based on the work of Wilhelm Wien) that energy is emitted and absorbed in distinct packets called "quanta" as early as the year 1900.[1] But the scientific community didn't embrace the idea seriously until another great physicist, Albert Einstein, made a similar assumption to explain the photoelectric effect in 1905. He worked on quantum mechanics for the next two years and proposed a model that could solve for the specific heat of solids, based on Planck's assumption that even the motion in his model is quantized.[2] He applied the Boltzmann statistical method to calculate the value of Planck's constant which matched the value that Planck had been using in his hypothesis. In the next two to three decades, strong foundations of the quantum theory were laid by many prominent scientists of that time including Niels Bohr, Werner Heisenberg, Louis de Broglie, Arthur Compton, Erwin Schrödinger, Max Born, John von Neumann, Paul Dirac, Enrico Fermi, Wolfgang Pauli, David Hilbert, Satyendra Nath Bose and many others. After the fifth Solvay conference in 1927, quantum mechanics emerged as its own field of study. Now theoretical chemistry that is known today is based on quantum mechanics.

What just began as theoretical chemistry in the early twentieth century is now a broad field that encompasses experimental quantum chemistry and theoretical/computational quantum chemistry. Experimentalists rely on different spectroscopic techniques like Raman Spectroscopy, infra-red (IR) spectroscopy, nuclear magnetic resonance (NMR) spectroscopy etc. Theoreticians use a variety of computational methods to test theories, make predictions and try to match them with the experiments. The interdependence of the theoretical and computational methods is very important as is their synergy. As soon as Schrödinger published his famous equation[3] in 1926, which needs to be solved in order to predict the properties of molecular systems, the scientific community responded with a flurry of critical publications that paved the way for computational chemistry. Heitler and London published the first theoretical treatment of the hydrogen molecule the very next year.[4] Conceptually, their valence bond model is still being used to date. This was followed by the development of the Hartree-Fock approximations[5,6] using molecular orbitals, the configuration interaction (CI) method,[7] perturbation theory[8] methods described by Møller and Plesset and even a paper describing multi-reference calculations[9] (a precursor to modern Multi-Configuration Self-Consistent-Field theory).

Despite all this, it was very difficult to implement the theories in practical applications as they required a tremendous amount of computational power, which was lacking. In 1929, Paul Dirac famously stated that "The fundamental laws necessary for the mathematical treatment of large parts of physics and the whole of chemistry are thus fully known, and the difficulty lies only in the fact that application of these laws leads to equations that are too complex to be solved".[10] This quote shows how much the times

have changed since 1929. Computing capabilities have improved by leaps and bounds. Back then, people believed that a diatomic system was as large a system as anyone could perform calculations on. Thankfully, that is no longer the case now due to the exponential growth of computational power available to scientists. In fact, Mulliken and Roothaan predicted that "Looking toward the future, it seems certain that colossal rewards lie ahead from large quantum–mechanical calculations of the structure of matter" in their famous "Broken Bottlenecks" article of 1959.[11] In 1984, Schaefer came out with a pronouncement that "We are confident that by the year 2000, essentially all fields of chemistry will acknowledge the accuracy of Mulliken and Roothaan's prophecy".[12] It is now reasonable to assume that something currently considered to be a herculean task and requiring massive amount of computational resources will be solved in minutes or even seconds, after a few decades.

The goal of this project is to use advanced theories and electronic structure methods to construct potential energy surfaces of molecules. These surfaces are crucial to any chemist who is trying to understand the finer details of molecular spectroscopy and the dynamics associated with it. However, it is important to understand the underlying electronic structure methods and various approximations involved before developing potential energy surfaces. Given a set of nuclei and electrons, the following calculations can be performed: (1) Locate the geometrical arrangements of nuclei that correspond to stable molecules. (2) Compute their relative energies. (3) Determine properties such as the dipole moment, polarizability, NMR coupling constants etc. (4) Calculate the rate by which one stable molecule can transform into another. In principle, all the properties of

molecular systems can be calculated if the Schrödinger equation is solved. However, it is a daunting task to solve the exact equation. The only systems that can be solved exactly (analytically) are one and two-body problems. Two-body problems are solved using the concept of a center of mass coordinate system and transforming the equations into two pseudo one-body problems. As the number of particles increase, there is no choice but to embrace numerical solutions, which can be obtained by performing mathematical operations iteratively. This is not to say that a numerical solution is a bad thing. In fact most of the methods being used currently, including the ones described in this thesis, revolve around numerical solutions. In principle many numerical methods are arbitrarily accurate and permit a numerically exact solution.

Several simplifying approximations are made. One of them is the Born-Oppenheimer (BO) approximation[13] that assumes that the behavior of electrons can be studied in a field of frozen nuclei. Since the nuclei (charge given by number of protons) and the electrons are attracted to each other via a pairwise Coulomb interaction, they exert corresponding forces on each other. However, since nuclei are many orders of magnitude heavier than an electron, their relative velocities can be considered negligible. The BO approximation takes advantage of this phenomenon and ignores the motion of the nuclei during the calculations. Essentially, the motion of the nuclei and the electrons are assumed separable enabling solution in the form of product wavefunctions. The BO approximation alone isn't sufficient to solve the Schrödinger equation; several other methods and theories like the variational method and perturbation theory are used to simplify it even further. The variational method[14] forms the basis for much of quantum chemical calculations

including the Hartree-Fock method, density functional theory (DFT) etc. It states that an approximate wave function has an energy which is equal to or above the exact energy. The equality holds true only if the wavefunction is exact. A flexible wavefunction is initially chosen to approximate the true wavefunction. Parameters in the trial wavefunction, like orbital basis set coefficients, can be varied to obtain different values of the energy. Since the energy obtained by this method can be at least equal to the exact energy, the parameters are varied to obtain the lowest energy possible. Perturbation theory, on the other hand, assumes that the wavefunctions and energies can be expanded in a series of terms (powers of the perturbation).[15] The basic idea of perturbation theory is that a small disturbance (perturbation) is added to a system for which the mathematical solution is known. The various physical quantities of the perturbed system are then expressed as corrections to the original.

Different computational methods are used to compute properties of molecular systems depending on the required accuracy of the calculations. In this thesis, the focus is on *ab initio*[16] quantum chemistry methods which are completely based on theory derived from first principles. In theory, *ab initio* methods eventually converge to the exact solution of the underlying equations as the number of approximations is reduced. However, in reality, it is not possible to eliminate all the approximations and hence some error always prevails. The main aim is to minimize this error and get as close to the exact energy as possible. Generally, the basis set[17] used to solve the Schrödinger equation is not complete. The basis set is a set of functions which are combined using the linear combination of atomic orbitals[18] (LCAO) method to create molecular orbitals. As the

basis functions tend towards the limit of a complete set, the errors get smaller and smaller. High quality data generated from *ab initio* methods are fit together using interpolative schemes to generate potential energy surfaces (PES). The concept of a PES arises from the BO approximation and is a representation of energy of a molecule as a function of its geometry. This is central to how chemists view molecular systems in terms of motion across a rich energy landscape where barriers separate wells corresponding to different stable structures.[19-45] The range of molecular distortions defines the potential energy surface. Developing global PESs is important as it forms a crucial step for quantum dynamics studies, which are used for understanding the system's properties. One limitation of using *ab initio* methods is the cost and poor scaling of the computation that is involved and so the calculations are limited to few-atom systems. More often than not, they require a tremendous amount of disk space, memory and computational time, depending on the system.

This thesis focusses on using highly accurate *ab initio* methods to generate a high quality PES for ozone. In order to develop a highly accurate potential energy surface, it is required to compute the potential energy of thousands of conformations corresponding to a wide array of molecular geometries. These energies are then fit together, using an interpolative scheme to form a surface. Rigorous calculations have been performed using the quantum chemistry package, MOLPRO[46] to obtain the data points used for fitting the surface and various schemes have been employed to get a smooth and accurate PES for the systems. Since the focus is on constructing reactive PESs, where bonds are formed and broken, multi-reference methods are required to describe the evolving wavefunction

connecting asymptotes with different electronic structures. Multireference methods include the different electron configurations that correspond to different bonding arrangements. Multi reference configuration interaction[47,48] (MRCI) methods are usually employed for this purpose. But as MRCI methods are very expensive to compute in terms of computational time, it is important that there are no discontinuities or unconverged data present while generating the surface. Discontinuities are undesirable especially for interpolative fitting methods. Convergence issues usually occur when a state switches its character along some coordinate due to crossings or avoided crossings of diabatic states. One of the most common ways to deal with this issue is to include the other relevant states with fixed relative weights with respect to the state of interest. This can be problematic as it is the weighted average energy of the states that is optimized, and convergence of the state of interest might be compromised. Also, there are chances of disruptions due to some excluded states. To avoid such problems, Deskevich *et al*. proposed the concept of dynamically weighting the electronic states (DW-MRCI) using an energy dependent functional, where $f(\Delta E) \propto 2/((\exp(-\beta*\Delta E) + \exp(\beta*\Delta E))^2)$.[49]

To understand how this method works, let us consider the six lowest singlet states of the BeOBe system, which is a triatomic molecule. We assume that the ground state is the state of interest. So in order to obtain accurate results for the ground state of this molecule, it must receive a larger weight when compared with the high lying excited states. This way, the crossings of the higher excited states are no longer disruptive. Using the dynamic weighting scheme, the excited states are assigned lower relative weights that are determined self-consistently at each individual geometry, as a function of their energy

gap between the states. So, if an excited state becomes degenerate with the ground state, the weights get adjusted according to the weighting scheme, enabling us to obtain in a balanced description of the orbitals.

a)

b)
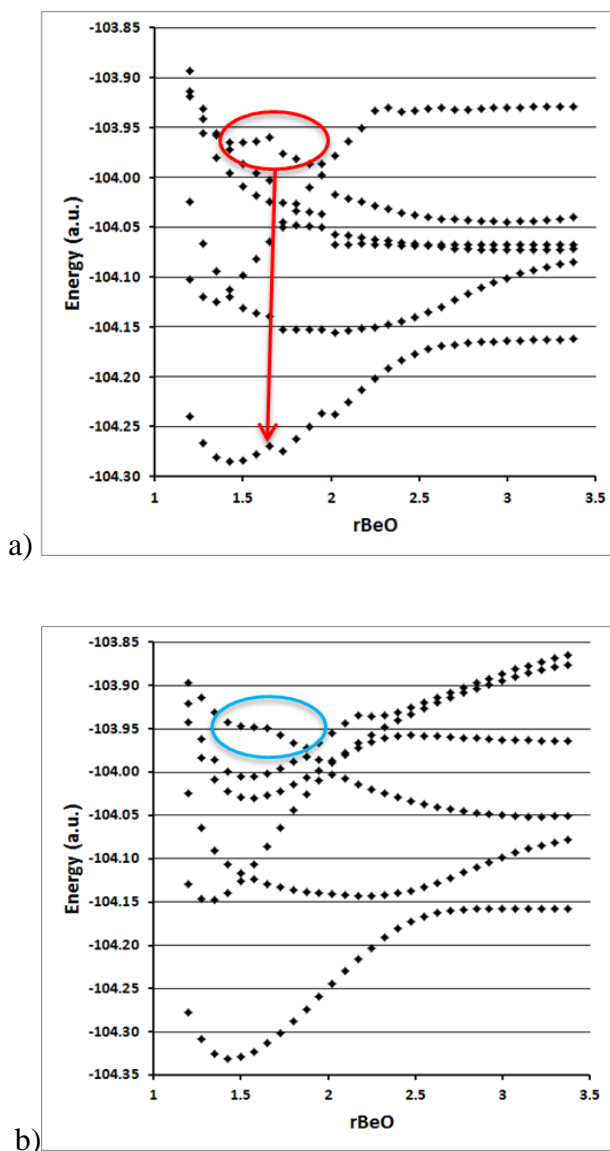
Figure 1.1 CASSCF calculations for the six lowest A_1 states for BeOBe, fixing the angle at 180°, done at the avdz level demonstrate the advantages of dynamic weighting. Fixed equal weights were used in part a). Dynamic weighting was used in part b), focusing the weight on the ground state. As highlighted above, it can be seen that the discontinuities that are caused by crossing with a still higher (neglected) state are avoided when the dynamic weighting scheme is implemented and the ground state is smooth and better converged.

Also, one might wonder about the need of a multi-state calculation when the state of interest is only the ground state. Sometimes when there are multiple states lying close to the state of interest, the states switch character which results in disruptions in the surface. This has been shown in the following figure, where the ground state switches character with the first excited state at rBeO = ~ 2.6 Å (highlighted in red). The disruption in the surface can be avoided by the inclusion of multiple states through the dynamic weighting scheme, making a seamless character switching.
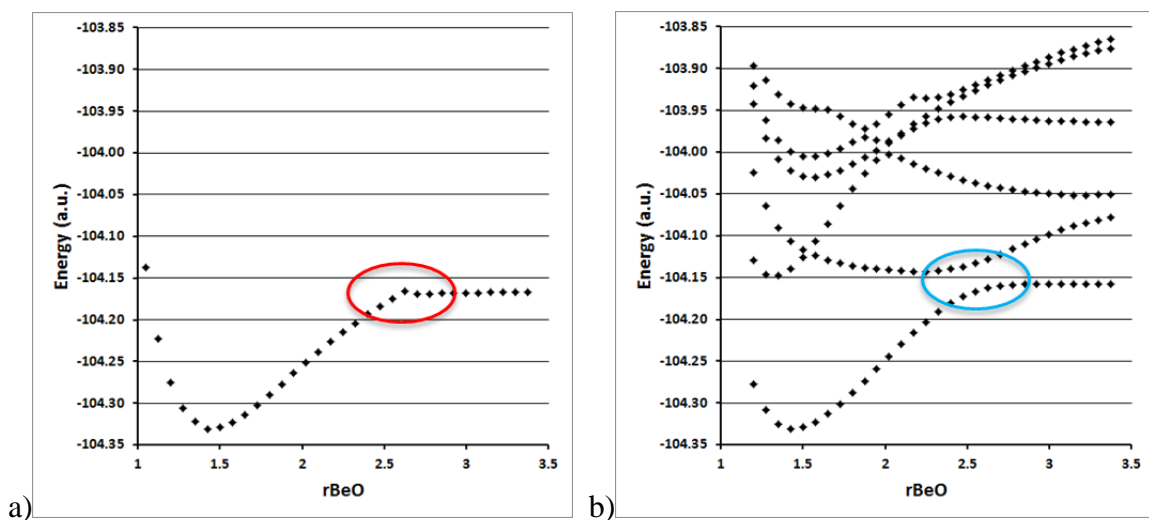
Figure 1.2 CASSCF calculations for BeOBe, fixing the angle at 180°, done at the avdz level demonstrate the importance of including multiple states. Part a) shows the surface obtained from a single state calculation. A disruption in the surface (highlighted in red) is apparent as the character switches with the first excited state. Including multiple states in the calculation using the dynamic weighting scheme, part b) results in a ground state that is well converged and the character switching is also seamless (highlighted in blue).

To summarize, *ab initio* methods have been developed by numerous scientists over the years to solve the Schrödinger equation approximately. Some methods are more accurate than others, but higher accuracy generally comes at the cost of higher computational effort. This thesis project makes use of very high accuracy methods, and

also develops schemes for dynamic weighting and curve/surface fitting. The purpose is to generate high quality potential energy surfaces so that they can be used for spectroscopic analysis and dynamics studies. The results and the future implications of the current work are discussed in the later sections.

2. BACKGROUND

O$_2$

O$_3$

(a)

(b)
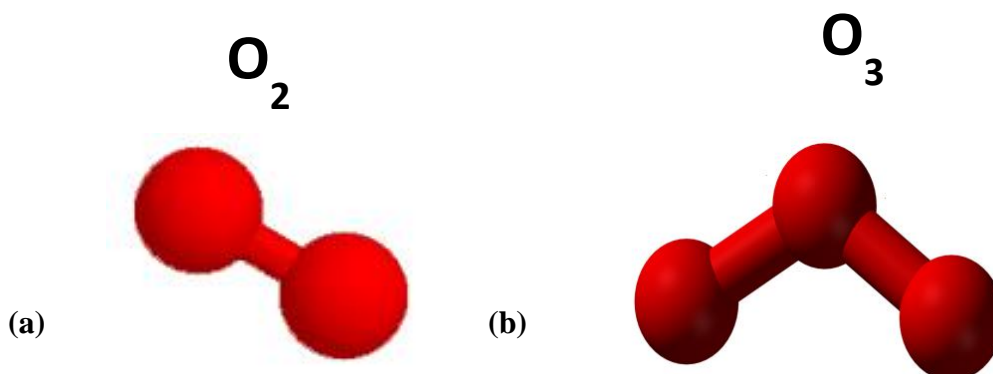
Figure 2.1 Physical structure of molecular oxygen and ozone. Part a) shows molecular oxygen which consists of two oxygen atoms, bonded covalently with a bond length of 121 pico-meters. Part b) shows an ozone molecule which consists of three oxygen atoms with a bond length of 127.2 pico-meters and a bond angle of 116.78 degrees. The presence of both these allotropes of oxygen in the earth's atmosphere is crucial for our survival.

Atomic oxygen (atomic number – 8) is one of most abundant elements by mass in the earth's biosphere. In fact, it is third most abundant element in the universe after hydrogen and helium. The oxygen that we breathe in is a diatomic molecule and consists of two oxygen atoms, as shown in figure 2.1 (a). Ozone is a triatomic molecule consisting of three oxygen atoms, as shown in figure 2.1 (b). While oxygen is a colorless and odorless gas at room temperature, ozone is pale blue in color and has a strong odor associated with it. It is mainly found in the stratospheric region of the earth's atmosphere. The earth's atmosphere can be classified into several layers. The lowest portion, the troposphere, extends from the earth's surface up to about 10 kilometers (km) in altitude. It accounts to about 80% of the atmospheres mass. In comparison, the tallest mountain on the planet, Mt. Everest, is only about 9 km high. The next layer, the stratosphere, continues from 10

km to about 50 km. As seen in the figure 2.2, most of the atmospheric ozone is concentrated in this layer.
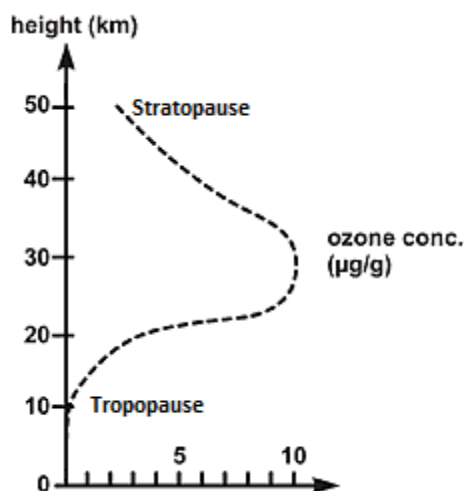
Figure 2.2 Ozone concentration in the atmospheric layers. The stratosphere is the layer between the tropopause and the stratopause. It is characterized by an increase of ozone with a maximum ozone concentration at about 30 km of height. Almost 99 % of the mass of the atmosphere is located within the lower 30 km.

Even though the overall concentration of ozone is very small in the atmosphere, it plays a crucial role in protecting the life on earth by shielding out most of the damaging, high energy ultraviolet (UV) rays.[50] The ozone layer absorbs a significant portion of the sun's radiation, preventing it from reaching the planet's surface. Most importantly, it absorbs the portion of ultraviolet light called UV-B. UV-B has been linked to many harmful effects, including various types of skin cancer, cataracts, and harm to some crops, certain materials, and some forms of marine life.[51]

O_2

$O_2+UV \rightarrow 2O$
(Slow)

$O+O_3 \rightarrow 2O_2$
(Slow)

$O_3+UV \rightarrow O+ O_2$
(Fast)

$O+ O_2 \rightarrow O_3+ heat$
(Fast)

O

O_3
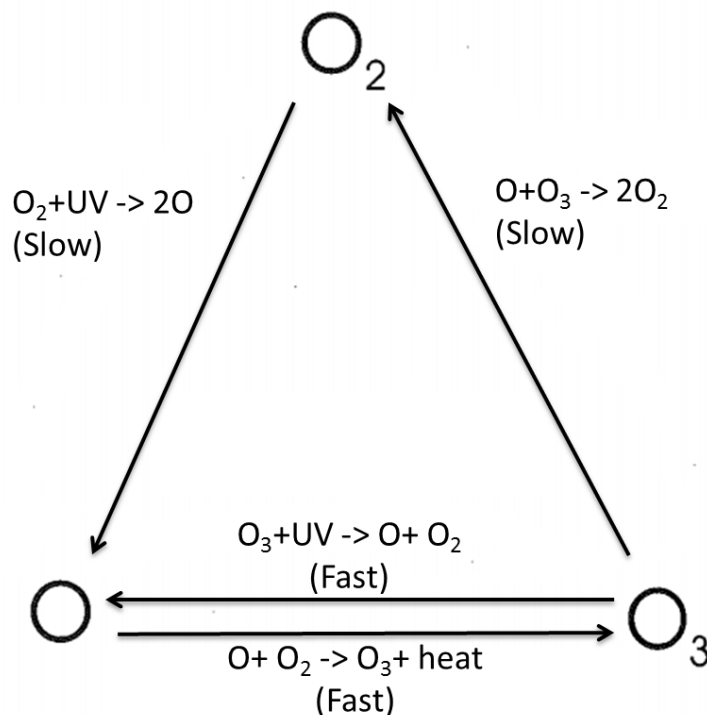
Figure 2.3 Chapman cycle - formation and destruction of ozone from molecular oxygen. Ozone is formed when molecular oxygen is split by UV radiation and the resultant oxygen atoms each combine with an oxygen molecule. Ozone is destroyed in the cycle when it combines with the oxygen atom to form two oxygen molecules.

At any given time, ozone molecules are constantly formed and destroyed in the stratosphere. This is explained by the Chapman cycle, proposed by a British mathematician and geophysicist, Sydney Chapman in 1930. He had proposed a pair of photochemical reactions that produce ozone, counter-balanced by a second pair of photochemical reactions that destroy it. Various approximations have been used to model the concentration of Ozone in the atmosphere over the years and are available in the literature.[52,53] But there are several discrepancies between the theory and experiment, making it difficult to accurately describe the formation and the dynamics of Ozone.[54,55] The recombination rate of O and O_2 (which is the intermediate step of the Chapman cycle) especially at low temperatures, the negative temperature-dependence of the isotope

exchange reaction[56-58] and the dissociation energy have not yet been accurately described even with the highest levels of calculations so far. This can be traced to the fact that there is a submerged reef-like barrier found in the asymptotic regions of some calculated PESs.

In fact, Schinke, Halberstadt et al proposed a modification to the ozone PES where the barrier was artificially removed and the rate constant was calculated.[54] His calculations showed that removing the barrier increased the total reaction cross-section and brought down the calculated rate constants to a better agreement with the experimental values. But in spite of using high levels of theory like multi-reference configuration interaction (MRCI) calculations with Davidson ($+Q_D$) or Pople ($+Q_P$) corrections along with large basis sets (up to sextuple zeta levels) which were extrapolated to the complete basis set (CBS) limit, the barrier could not be removed from the surface. Hence, this modification was dismissed as it didn't have the electronic structure theory backing its claim although all the kinetics experiments suggested otherwise.

Since it is clear that the potential energy surface is sensitive to the details of the calculations, the ozone system has been studied much more carefully using multi-state MRCI methods. It is shown that the minimum energy path is indeed barrier-less, resulting in kinetics in much better accord with the experimental results.

3. ELECTRONIC STRUCTURE CALCULATIONS

Performing an electronic structure calculation can be broken down into two major steps –

(1) Preparing an input file specifying the details of the calculation

(2) Running the calculation.

Electronic structure calculations are different from other forms of modeling because they are *ab initio* (based on first principles). It means that the calculations do not contain any external parameters other than the fundamental ones (e.g., electron mass) used to describe the system. These kinds of calculations enable researchers to make predictions without referring to the corresponding experiments. This is extremely useful in studying systems for which no experimental data is available. As mentioned in the previous sections, this is done by solving the Schrödinger equation within the Born-Oppenheimer (BO) approximation. Since the nuclei are assumed to be fixed, while we solve for the electronic motion, one must first define the molecular geometry (i.e. the position of all the atoms) in the input file that is to be submitted for the calculation. Since MOLPRO does not have an interface to build a molecule, all the molecular geometries must be inputted in either Cartesian coordinates or in *Z-matrix* form. The electronic energy as a function of the $3N$-6 internal nuclear degrees of freedom (for N nuclei) defines the potential energy surface. Also, since the Schrödinger equation cannot be solved directly, the wavefunction is represented by basis sets and hence solving the equation numerically. The actual running of the calculation depends on the algorithms used, the way the

software is compiled and available computational resources. In order to obtain results, the theoretical methods must be transformed into working computer programs. Since different algorithms exhibit different behaviors, it is important to evaluate whether a certain type of calculations can be carried out with the available resources.

All the electronic structure theory in this thesis is based on the Hartree-Fock (HF) theory. It is a very common *ab initio* method that is implemented by computational chemistry programs. In older literature the HF method was also called the self-consistent field (SCF) method. According to HF theory, the molecular orbitals can be determined as eigenfunctions of a set of one-electron operators. The objective is to find an optimal set of functions for each electron, treating the electron correlation energy in an average way and solve the Schrödinger equation to get the energy of the system. The wavefunction is described in the input file with the number of electrons, symmetry state and the spin of the system. In this work, all the HF calculations have been done for the *highest spin*. This is because when ozone dissociates into fragments, both the fragments have triplet spin which can be combined to give singlets, triplets and quintets. Although the ground state of interest is a singlet, for the preliminary HF calculation performing the quintet ensures smooth dissociation. It is important to note that the HF method cannot provide an exact solution to the Schrödinger equation for systems that have more than one electron, irrespective of the basis used. Nevertheless, it is a starting point for most of higher methods (called post-HF methods) where the electronic correlation is added to the HF solution by including additional determinants in the calculations that lead to the exact solution. Multi-configurational self-consistent field (MCSCF) method is a very common

post HF method which uses a combination of configuration state functions (CSF) to approximate the electronic wavefunction. In MCSCF method, both the orbitals and expansion coefficients are simultaneously optimized using a set of CSFs to describe the wavefunction. One case of MCSCF method is the complete active space self-consistent field (CASSCF) method, where the CAS expansion is obtained by including all possible CSFs within a chosen *active space* of orbitals. Even though it is better than HF method to describe the electronic wavefunction, the CASSCF method still misses most of the dynamic correlation. So a CASSCF calculation is usually followed by a Configuration Interaction (CI), or a perturbation calculation to add the correlation energy. In this project, multi-reference configuration interaction[59,60] (MRCI) methods are used. The MRCI method is built upon the CASSCF and accounts for both dynamical and non-dynamical correlation effects. Most of the time, poor computational scaling limits its usage to small molecular systems. But it has been shown that this method has been very accurate, especially when it comes to describing systems where the electronic states exhibit strong multi configurational effects. MOLPRO considers single and double excitations in its MRCI procedure. To make up for the lack of size extensivity due to lack of triple and higher excitations, we add a correction factor to our calculations called the Davidson correction[61] ($+Q_D$).

To accurately fit a potential energy surface that describes the formation of ozone, one must first understand how many electronic states of ozone must be included in the calculations. The ground state of ozone is a singlet, which means that the total spin of the system is zero. Doublet and triplet states refer to the electronic states where the total spin

is ½ and 1 respectively. The ground state dissociates adiabatically to triplet states of molecular and atomic oxygen. Schinke's MRCI calculations include only the ground ^{1}A' state in the CASSCF reference. This can be assumed to be a good strategy as the excited states of ozone are very high in energy and well separated from the ground state. But as we approach the asymptotic regions, this leads to problems as we have the excited states that are excluded in the calculations becoming degenerate with the ground state resulting in root flipping and other convergence problems. Hence, we need to include more states in the calculations in order to get a smooth and well behaved surface. C_S symmetry was used to describe the molecule. It is a lower symmetry group with only a mirror plane as the symmetry element. In C_S symmetry, the adiabatic dissociation can be represented as follows:

$$O_3 \, (^1A') \rightarrow O_2\left(^3\Sigma_g^-\right) + O \, (^3P_g)$$
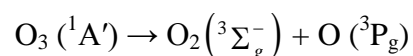
The electronic states are also assigned to be gerade (even in German) and ungerade (odd in German), based on its reflection through an inversion center. A wavefunction is considered gerade if there are even number of electrons in its ungerade orbitals. If it there are an odd number of electrons in its ungerade orbitals, it is considered ungerade. The $\left(\Sigma_g^-\right)$ corresponds to (A″) and (P_g) corresponds to (A′ + 2A″), combining to give (2A′ + A″), a three-fold degeneracy of states. Schinke included these three states with equal weights to describe his asymptotic region of the surface. But as mentioned earlier, due to an avoided crossing with an excited state, the ground state switches its character with the excited state along the path of dissociation. The barrier reef that is observed in some calculations was determined in our study to be due to an avoided crossing between the

ground state in the molecular well and the lowest excited ^{1}A' state. Diabatically, the ground state of ozone correlates to excited states of both the atomic and molecular oxygen as follows:

$$O_3\,(^1A') \rightarrow O_2\left(^1\Delta_g\right) + O\,(^1D_g),$$
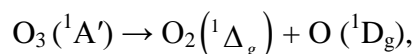
where $\left(\Delta_g\right)$ corresponds to (A' + A''), and (D$_g$) corresponds to (3A' + 2A''). Both of them combine to give (5A' + 5A''), a ten-fold asymptotic degeneracy of the excited states. Therefore 13 singlet states were considered relevant for the calculations (7A', 6A'') to ensure a smooth and robust ground state for ozone.

One of the main issues of including multiple states with fixed weights is the convergence of the state of interest. If fixed weights are used to describe any system, it can be difficult to get smooth wavefunctions describing the system across all geometries. This issue is tackled by using a dynamic weighting scheme, using an energy dependent functional. Using this scheme, the state of interest is given the maximum weight and all the other states are assigned weights self-consistently based on their energy difference with respect to the state of interest. Degenerate states will have equal weights. If the difference in energy of a particular state is too high, then it will automatically receive a smaller weight and vice-versa ensuring a smooth switching of character as we move towards the asymptotic regions. This way, the wavefunction evolves smoothly across the PES while also preserving the asymptotic degenerate patterns. The initial Hartree-Fock (HF) calculations were performed using the Dunning AVTZ basis set.[62] Next the HF orbitals from the previous step were used as the initial guess for a series of DW-SA-

CASSCF iterations (also using the AVTZ basis). For the DW-SA-CASSCF calculations, 13 singlet states (7 A', 6 A'') were initially assigned equal weights. The 2s orbitals were closed in all of the weight determining iterations. The energy dependent functional used for dynamic weighting was set to 3.0 eV. The SA-CASSCF energies computed in the second iteration tend to differ slightly from those of the first iteration as the weights get updated. A series of iterations are then performed until the energy of the state of interest (in this case the ground state) changes by less than 10^{-6} a.u. This value is set by the user and it defines the tolerance that is expected in each calculation. Tests have found that achieving self-consistency to the level of 10^{-6} a.u. in the DW-SA-CASSCF calculation results in stability in the subsequent MRCI calculation of ~10^{-7} a.u. At each particular geometry, weights are determined at the DW-SA-CASSCF level. The DW-SA-CASSCF procedure has been found to converge more robustly when performed in the configuration state function (CSF) basis (MOLPRO option *config,csf*). This option is not currently available in Molpro when more than one spin-multiplicity is included, but in those cases it is often helpful to start with one spin-multiplicity and the CSF basis and then introduce states with other spins in a second step. Here we consider only the singlet states. MRCI calculations have been performed using different basis (AVnZ, n=3-6) along with different Davidson corrections and finally extrapolated to give us the CBS extrapolated energies.

4. RESULTS

Three equivalent global minima of ozone are of C_{2v} symmetry ($r_1 = r_2 = 2.4052$ a.u., $\theta = 116.75°$), a higher energy high-symmetry (D_{3h}) minimum also exists, while points along the minimum energy dissociation path are of C_S symmetry. Upon dissociation the asymptotic experimental bond distance for O_2 is 2.2819 a.u.[63]

A minimized path for dissociation was calculated in valence coordinates at the MRCI(+Q_D)/CBS level using numerical optimization to relax the second O-O bond distance and the O_1-O_2-O_3 angle (θ) directly on the CBS surface. The procedure includes a 13 state (7 $^1A'$ + 6 $^1A''$) DW-SA-CASSCF calculation as a reference for MRCI(+Q_D) calculations of the lowest $^1A'$ state. To estimate the path, the 2s orbitals were closed in the CASSCF reference but correlated in the MRCI(+Q_D) calculation. At each step in the optimizations, MRCI(+Q_D) energies obtained with AVTZ and AVQZ bases were extrapolated to the CBS limit using the l^{-3} formula.[64] The rO_1O_2 distance was scanned out to a distance of 20 bohr relaxing the other two coordinates at each step starting from the global minimum (optimized at this level). A plot of energies along the path is shown in Figure 4.1 and optimized parameters are listed in Table 4.1.

Table 4.1 Geometric parameters along a relaxed dissociation path.

rO_1O_2 (a.u.)	rO_2O_3 (a.u.)	θ (degrees)	Energy (kcal/mol)
2.398	2.398	117.01	0.00
2.600	2.357	116.13	3.56
2.800	2.322	115.58	10.34
3.000	2.296	115.30	16.87
3.150	2.283	115.15	20.65
3.300	2.275	115.05	23.25
3.450	2.272	115.03	24.82
3.600	2.271	115.12	25.64
3.750	2.271	115.29	25.97
3.900	2.272	115.57	26.05
4.050	2.273	115.86	26.00
4.200	2.274	116.19	25.90
4.350	2.275	116.51	25.82
4.500	2.276	116.83	25.76
4.650	2.277	117.12	25.74
4.800	2.277	117.38	25.74
4.950	2.278	117.59	25.76
5.200	2.278	118.18	25.82
5.500	2.279	116.85	25.90
6.000	2.279	115.80	26.03
7.000	2.279	113.52	26.22
20.000	2.279	---	26.38

Note that for the calculations whose results are listed in Table 4.1 and plotted in Figure 4.1 only one state was included in the MRCI calculation, the default *relaxed reference* Davidson correction was applied, and the 2s orbitals were closed in the DW-SA-CASSCF reference. All of these choices affect the characteristics (and even existence) of the barrier. The relaxed angle does not vary significantly along the path and for $rO_1O_2 \geq 3.3$ a.u., rO_2O_3 has relaxed close to its long range asymptotic value. Therefore to investigate the sensitivity of the barrier to details of the calculations, a series of 1D scans were performed for $rO_1O_2 \geq 3.3$ a.u. holding rO_2O_3 and θ fixed at 2.2819 a.u. and 116.75° respectively (experimental geometric parameters for O_2 and O_3).
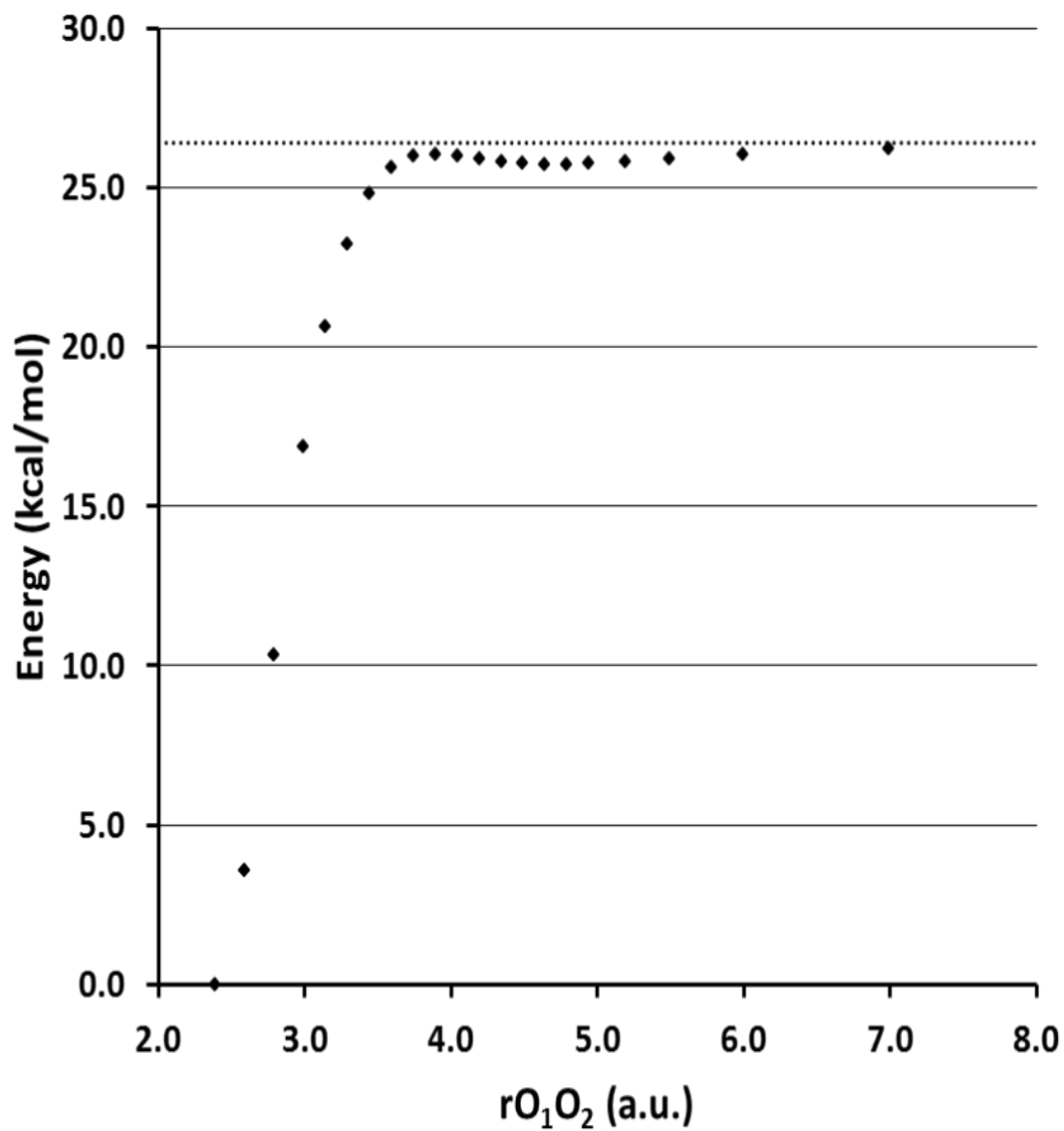
Figure 4.1 Relaxed dissociation path for ozone showing submerged reef barrier and vdW well obtained in single-state MRCI calculation with relaxed-reference Davidson correction and 2s orbitals closed in 13-state DW-SA-CASSCF reference.

The effects of basis set completeness and choice of active space in the CASSCF reference for MRCI energies in the transition region are shown in Figure 4.2.

a)

b)
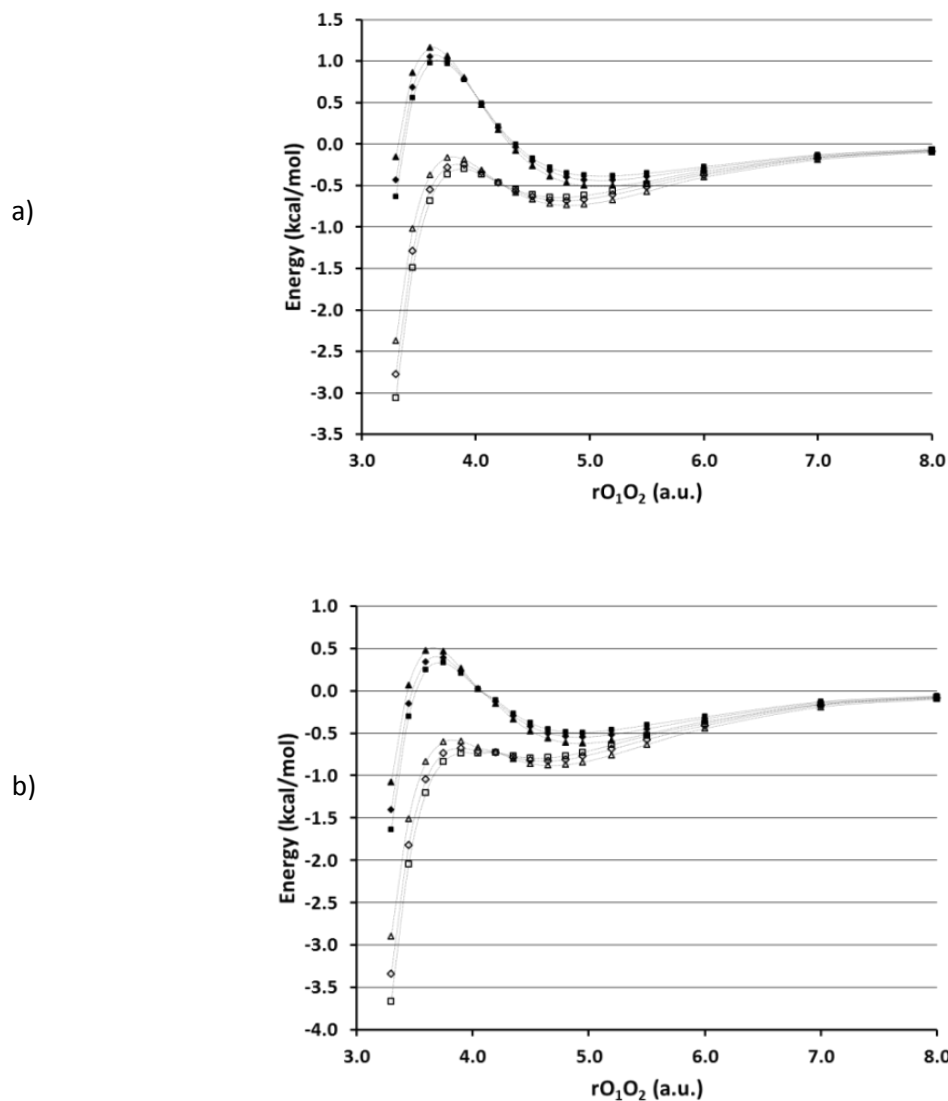
Figure 4.2 Cut through transition region showing reef barrier obtained in single-state MRCI calculation (filled symbols) and with relaxed reference Davidson correction (open symbols). a) 2s orbitals closed in the 13-state DW-SA-CASSCF reference. b) full-valence active space in 13-state DW-SA-CASSCF reference. Energies are compared for avtz (triangles), avqz (diamonds) and CBS(avtz,avqz) (squares) basis sets.

Although the 2s orbitals remain very nearly doubly occupied in the full-valence reference, opening them has a significant effect on the barrier seen in the MRCI energies (barrier is lower for full-valence, compare Figures 4.2a and 4.2b). The vdW well and the reef barrier both become less pronounced with larger basis sets, but do persist in the full-valence CBS result. The barrier is not submerged without the Davidson correction.

Next the effect of including a second A' state in the MRCI calculation is shown in Figure 4.3 (at the CBS level, based on a full-valence 13-state DW-SA-CASSCF reference).
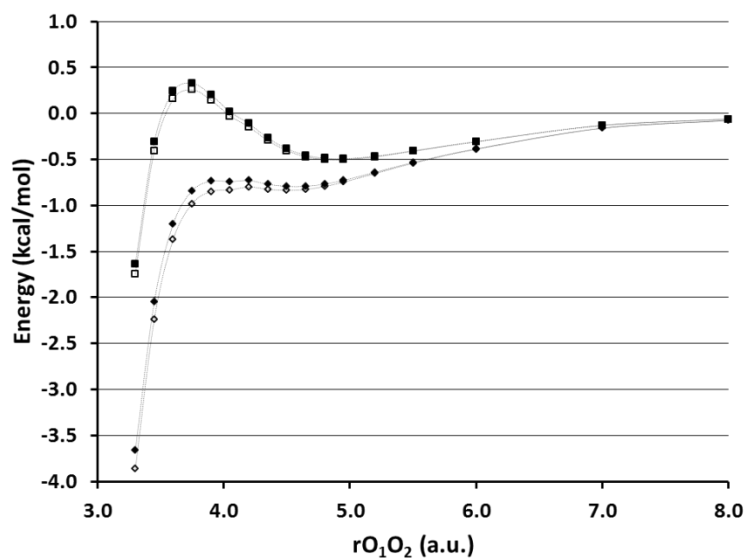
Figure 4.3 Cut through transition region showing reef barrier obtained in single-state MRCI calculations (filled symbols) and two-state MRCI calculations (open symbols). MRCI energies (squares) and with relaxed reference Davidson correction (diamonds). A full-valence active space was used in a 13-state DW-SA-CASSCF reference. Energies are compared at the CBS(avtz,avqz) level.

Slight mixing was obtained in the two-state MRCI calculation which has a significant effect on the barrier. After applying the relaxed reference Davidson correction to the two-state MRCI energy at the CBS level, the barrier has all but disappeared (lowest curve in Figure 4.3). A consequence of using two or more reference states in the MRCI is a change in the internal contraction. Our tests with up to 7 A' states in the MRCI indicate that no significant mixing occurs beyond the second state and no further qualitative change occurs by including more than 2 states.

Since the barrier depends qualitatively on the Davidson correction we explore the role of different implementations of the Davidson correction and analogous Pople corrections. The standard Davidson correction scales the correlation energy in an MRCISD calculation to account for lack of rigorous size extensivity which arises due to the limitation of excitations to singles and doubles. Thus it is said to approximately account for higher excitations. The standard correction scales the correlation energy based only on the weight of the initial MCSCF vector. Hoffmann and coworkers recently published a *modified* Davidson correction that scales the correlation energy based on the total weight of all reference CSFs in the normalized MRCISD wavefunction.[65] It was pointed out that although the difference between the standard and modified corrections is usually small it can be significant in the region of avoided crossings, and produce smaller errors in PESs relative to full-CI. The MOLPRO package computes *relaxed* and *rotated* Davidson corrections for multistate MRCI in addition to the standard (or fixed-reference) correction. The rotated correction is based on rotated reference functions (obtained by projection and ortho-normalization) designed to maximize overlap of the reference

functions with the MRCI wavefunction. The rotated correction has been reported to improve the accuracy of PESs in the region of avoided crossings. A comparison of the relaxed and rotated Davidson corrections is shown in Figure 4.4. Significantly, the rotated correction produces a path through the transition region that is barrierless and monotonically decreasing in energy. The fixed-reference and Hoffmann's modified Davidson corrections also produce barrierless cuts that are indistinguishable from the rotated correction in Figure 4.3. It is only the relaxed correction for which a small barrier persists. The analogous Pople corrections (fixed, relaxed and rotated) produced energies (not shown) for this cut that are qualitatively similar to their Davidson counterparts.
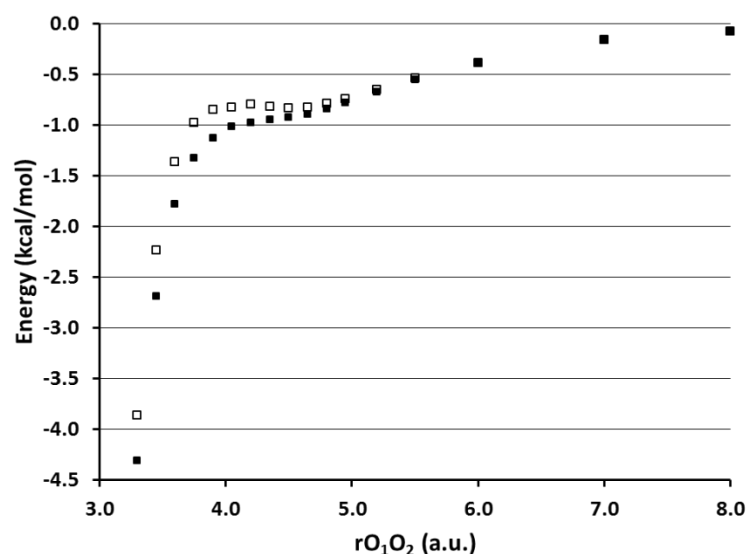
Figure 4.4 Cut through transition region comparing rotated reference (filled symbols) and relaxed reference (open symbols) Davidson corrections for two-state MRCI calculations. A full-valence active space was used in a 13-state DW-SA-CASSCF reference. Energies are compared at the CBS(avtz,avqz) level.

All of the results shown in Figures 4.1 to 4.4 are based on MRCI calculations using a 13-state dynamically weighted DW-SA-CASSCF reference. Figure 4.5 compares the

results obtained with the 13 weights fixed at their long range asymptotic values. For the choice of weighting parameter ($B = 3.0$ eV) used in these calculations, the asymptotic weights of the three lower states is 1.0 while the 10 excited states receive relative weights of ~0.4. Also compared in Figure 4.5 is the effect of including only three states (with fixed equal weights) instead of 13. As seen in Figure 4.5, fixing the weights in the 13-state calculation has no appreciable effect on the MRCI energies in the barrier and vdW regions. At the two shortest distance data points (entering the well) the dynamic weighting scheme is seen to improve convergence of the ground state slightly as it designed to do (only those two data points are visible in the plot as the difference is negligible for the other points). However, including only three states in the CASSCF reference has a more pronounced effect, the disruption arising from switching character with excluded states.

The dissociation energy of ozone has been another discrepancy between theory and experiment. In Table 4.2 MRCI based dissociation energies with valence electron correlation are listed for triple- through sextuple-ζ bases (AVnZ, n=3-6) computed at the experimental geometries of ozone and O_2 (O + O_2 was treated as a supersystem at 25 Angstroms separation). Three sets of CBS energies were computed using the l^{-3} formula and energies from the AVTZ and AVQZ bases (CBS34), the AVQZ and AV5Z bases (CBS45) and with the AV5Z and AV6Z bases (CBS56). In addition to the l^{-3} extrapolations, another CBS strategy was tested for which the reference and correlation energies from all available basis sets were separately extrapolated using an optimized power-law: $E_{lmax} = E_{CBS} + Al^{pow}$. Core-valence corrections (CV) were estimated from all-

electron calculations using either l^{-3} CBS extrapolation with cc-pw-CVQZ and cc-pw-CV5Z bases (increasing the dissociation energy by 32 cm^{-1}), or optimized power-law extrapolation using the cc-pw-CVTZ, cc-pw-CVQZ and cc-pw-CV5Z bases (increasing the dissociation energy by only 9 cm^{-1}). Scalar relativistic (SR) effects were estimated using the Douglas-Kroll-Hess 8th-order Hamiltonian. CBS extrapolation of energies from the AV5Z and AV6Z bases using the l^{-3} formula, or optimized power-law extrapolations of triple- through sextuple-ζ bases (AVnZ, n=3-6), both lowered the dissociation energy by 21 cm^{-1}. Finally the spin-orbit effect lowers the dissociation energy by 79.3 cm^{-1}.
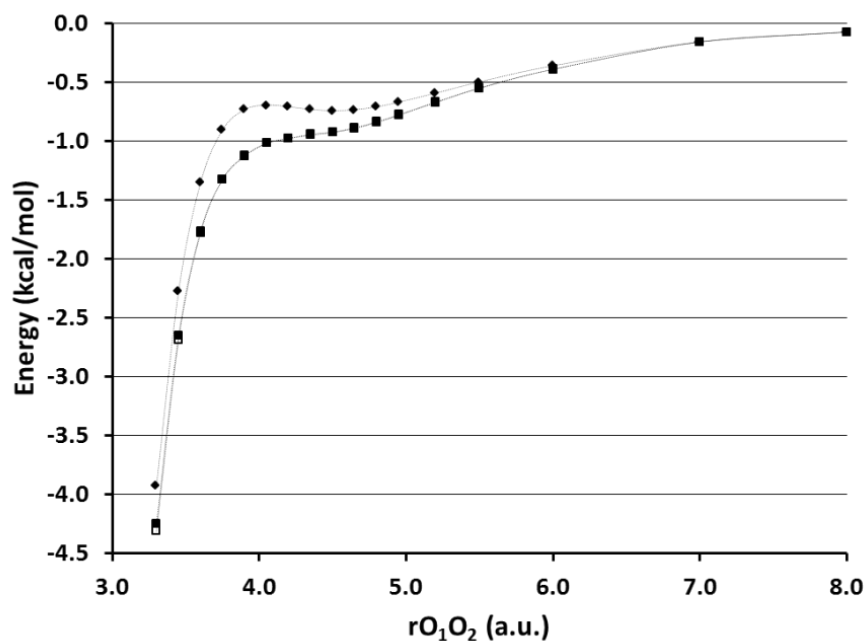
Figure 4.5 Cut through transition region comparing rotated reference Davidson-corrected two-state MRCI energies. A full-valence active space was used for a three-state SA-CASSCF reference (filled diamonds) with fixed equal weights, a 13-state fixed weight SA-CASSCF reference (filled squares), and a dynamically weighted 13-state DW-SA-CASSCF reference (open squares). The 13-state DW-SA-CASSCF results are only distinguishable at the two shortest distances. MRCI energies are compared at the CBS(avtz,avqz) level.

Table 4.2 Calculated dissociation energies (cm^{-1}) for MRCI and with applied relaxed or modified Davidson corrections.*

Method	AVTZ	AVQZ	AV5Z	AV6Z
MRCI	7926.6	8522.7	8687.6	8767.5
MRCI(+Q$_{rel}$)	8099.1	8786.6	8980.0	9070.7
MRCI(+Q$_{mod}$)	8108.2	8798.0	8992.1	9083.2

Method	CBS34	CBS45	CBS56	CBS_pow
MRCI	8957.6	8860.7	8877.3	8857.0
MRCI(+Q$_{rel}$)	9288.4	9182.9	9195.3	9171.6
MRCI(+Q$_{mod}$)	9301.3	9195.8	9208.3	9184.5

Method	CBS34+ CV+SO+SR	CBS45+ CV+SO+SR	CBS56+ CV+SO+SR	CBS_pow+ CV+SO+SR
MRCI	8889.2	8792.3	8808.9	8765.7
MRCI(+Q$_{rel}$)	9220.0	9114.5	9127.0	9079.8
MRCI(+Q$_{mod}$)	9232.9	9127.4	9139.9	9093.2

* Best experimental estimate 9234.1 cm^{-1}. CBS34, CBS45, CBS56 and CBS_pow refer to different basis set extrapolations while CV, SO and SR refer to core-valence, spin-orbit and scalar relativistic corrections.

The best current estimate of D_0 for $O_3 \rightarrow O_2 + O$ is 8563.6 ± 3.5 cm^{-1}. Using 1457.7 and 787.2 cm^{-1} for the ZPEs of O_3 and O_2 respectively results in an estimated D_e of 9234.1 cm^{-1}. There is more than 3.5 cm^{-1} uncertainty in D_e due to uncertainty in the ZPE of ozone. D_e is certainly underestimated without Davidson corrections even at the CBS

level. With Davidson corrections and various CBS extrapolations, calculated values for D_e vary by about 150 cm^{-1}, with the largest value (MRCI(+Q$_{mod}$)/CBS34) coming within experimental error. Near exact agreement came from the simple l^{-3} extrapolation of the smaller triple and quadruple zeta bases, whereas CBS extrapolations of the largest bases with the l^{-3} formula or separate power-law extrapolation of the correlation energy produce values for D_e that are further from experiment. From these results, it appears that the largest remaining uncertainties lie in the CBS extrapolations and the Davidson correction. The significance of Davidson corrections also confirms the importance of higher-order correlation effects.

5. CONCLUSIONS AND REMARKS

One might think that theoretical chemistry is all about using computers to model or simulate molecular behavior. But as seen in the previous sections, we can now say that such an assumption is only partly true. Theoretical chemistry does involve computer calculations and simulations but it also involves analytical theory, which deals with how the algorithms are developed from the fundamental equations. It involves relating the macroscopic properties of molecular systems with their corresponding microscopic properties at the molecular level. Essentially, theoretical chemistry has evolved into a vast field that encompasses mathematics, physics and computers up to a certain degree to explain the behavior of various molecular systems from a fundamental point of view. It is also used to extend our knowledge by analogy to similar systems. For example, the $O + O_2$ reaction to form O_3, is qualitatively similar to the $OH + O_2$ reaction to form HO_3 from an electronic structure standpoint. Like Ozone, HO_3 is an important molecule in the atmosphere, potentially affecting the concentration of free OH. The OH concentration is critical for models of atmospheric chemistry. Scientists around the world are interested in studying the formation of these molecules and the dynamics associated with them. Until recently, it has been difficult to describe the dynamics of such systems because of the challenges associated with generating accurate potential energy surfaces. Recent experiments indicate that the formations of both the molecules must be barrier-less. This has been a challenge for theory, but is now confirmed for ozone in the first paper of this thesis. Future work is focused on developing a highly accurate global potential energy surface for the HO_3 molecule. This will result in more realistic studies of the molecular systems so that they are better understood.
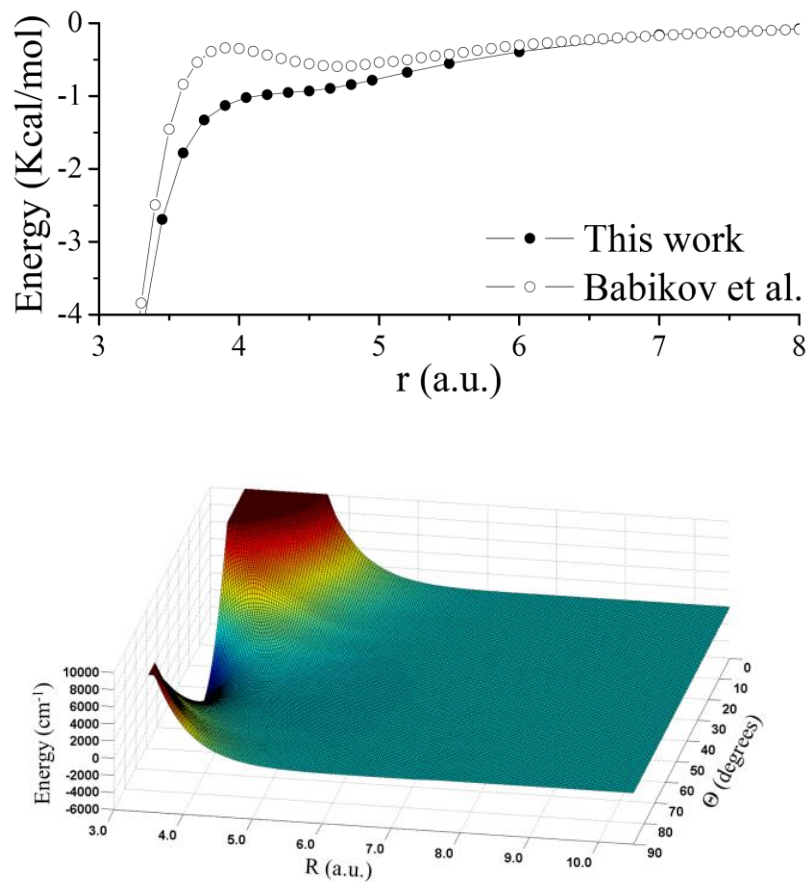
Figure 5.1 Upper panel: minimal energy path for O_3 formation along an O-O bond length obtained in this work (filled circles) and its comparison with that on the hybrid PES of Babikov et al.[63] (open circles). Lower panel: the corresponding two-dimensional potential energy surface in the O-O_2 Jacobi coordinates.

The electronic structure methods demonstrated in this work helped in characterizing a more accurate potential of ozone. The new potential energy surface, thus calculated resulted in a dissociation energy which is in good agreement with the experimental values. Also, more importantly, the reef-like barrier that was found in all the previous calculations is absent in this surface as the avoided crossing between electronic states have been well-represented. This can be seen in the figure 5.1. It automatically improved

the calculated values of the rate constant for the $O+O_2$ exchange reaction and we can depict the negative temperature dependence as observed experimentally. All the work that has been reported in the thesis so far is but the first step in our quest to understanding these systems in greater detail than before. The next step after developing the accurate surfaces is the quantum wave-packet studies that can be performed using the surfaces and comparing how well the dynamical theory fares against the experiments. The methods described in this work are only going to get better in the future as they are further developed and refined.

It is interesting to note the development of theoretical chemistry over the years. Initially, it was just the experimentalists who were dwelling on different aspects of theory to explain their experimental work. Slowly over the past few decades, there have been people who started focusing exclusively on developing new theory – new concepts, new equations, new computational tools etc. and now both theoreticians and experimentalists work together solving problems. Before I conclude my thesis, I would like to mention the vast improvements that have been made in computational power of modern day computers and how it has been instrumental in allowing scientists to develop better methods and approximations to improve their theories. High speed computing has come a long way in the past few decades in ways that no one could have imagined before. Dr. John Von Neumann, a noted computer scientist and a pioneer of the application of operator theory to quantum mechanics, made the following statement back in 1949 – "It would appear we have reached the limits of what is possible to achieve with computer technology." But he immediately and prudently added that, "One should be careful with

such statements; they tend to sound pretty silly in five years." That pretty much sums up everything when it comes to the advances that are being made in the field of computational studies.

Our computational capabilities are indeed rising exponentially as proposed by inventor and futurist, Raymond Kurzweil, in his recent book – "The Singularity Is Near". However, it is not just computers that have improved with time, the computational algorithms for performing quantum dynamic calculations have been improving even faster. In fact, the total advancement in our capabilities since the first computers owes more to the development of methods and algorithms than to increases in raw CPU cycles. These factors will continue to have a tremendous impact on all of the scientific community, leading toward a broader understanding of theoretical chemistry and how it fits into our everyday lives. Given the vast number of interesting research problems in this field coupled with the ever improving tools of quantum mechanics, I think there will be a day in the future where derivatives of procedures described in this thesis will have become the norm for calculating the properties of any molecular system.

APPENDIX A

COMMUNICATION: HIGHLY ACCURATE OZONE FORMATION

POTENTIAL AND IMPLICATIONS FOR KINETICS

A. COMMUNICATION: HIGHLY ACCURATE OZONE FORMATION POTENTIAL AND IMPLICATIONS FOR KINETICS

Richard Dawes,[1,*] Phalgun Lolur,[1] Jianyi Ma,[2] and Hua Guo[2,*]

[1]Department of Chemistry, Missouri University of Science and Technology, Rolla, Missouri 65409;

[2]Department of Chemistry and Chemical Biology, University of New Mexico, Albuquerque, New Mexico 87131

Emails: dawesr@mst.edu, hguo@unm.edu

ABSTRACT

Atmospheric ozone is formed by the $O + O_2$ exchange reaction followed by collisional stabilization of the O_3^* intermediate. The dynamics of the $O + O_2$ reaction and to a lesser extent the O_3 stabilization depend sensitively on the underlying potential energy surface (PES), particularly in the asymptotic region. Highly accurate Davidson corrected multistate multireference configuration interaction calculations reported here reveal that the PES for the formation of O_3 from $O + O_2$ is a monotonically decaying function of the atom-diatom distance and contains no ″reef″ feature found in previous *ab initio* calculations. The absence of a submerged barrier results in an exchange rate constant with the correct temperature dependence and in better agreement with experiment, as shown by quantum scattering calculations.

The ozone layer protecting Earth from harmful UV radiation is formed by reactions of molecular oxygen, $O_2(^3\Sigma_g^-)$, with atomic oxygen, $O(^3P)$, which is generated by photodissociation of O_2. However, the detailed kinetics and dynamics of this seemingly simple chemical reaction are still not well understood. One of the fascinating aspects of ozone chemistry is the discovery of selective enrichment of heavy ozone isotopomers in the atmosphere and in laboratory settings.[1-2] This so-called mass-independent fractionation (MIF) effect is at odds with the normal mass-dependent isotope effect,[3-5] highlighting the complicated mechanisms for the reaction and energy transfer in ozone formation. Convincing evidence has recently emerged from both experimental and theoretical studies that the ozone MIF is likely to originate from zero-point energy (ZPE) differences between different O_2 isotopomers involved in the $O + O_2$ exchange reaction,[6-12] underscoring the quantum nature of the process. So far, however, there has not been any first principles model that can explain the MIF in a satisfactory fashion.

One of the major obstacles in our understanding of the ozone chemistry is the lack of a quantitatively accurate potential energy surface (PES).[13] While the ground electronic state of $O_3(X^1A')$ near its C_{2v} minima is well separated from low-lying excited states, the asymptotic regions of the PES involve interaction with many low-lying excited electronic states. Due to the multi-reference nature of the system in these regions, it was only recently that reasonable agreement has been achieved between the calculated and measured dissociation energies of O_3.[14-16] Even the most recent O_3 global PES[17] based on multi-reference configuration interaction (MRCI) data[16,18] still requires empirical adjustments to match the experimental dissociation energy.

High-level *ab initio* calculations have found an interesting feature in the O + O_2 asymptotic region of the O_3 PES: a saddle point exists along the formation pathway of O_3, but beneath the dissociation limit.[16,18] This small submerged ″reef″ separates the deep O_3 chemical well from a shallow van der Waals well. Since its discovery, this feature has been found in *all* high-level *ab initio* calculations up to the complete basis set (CBS) limit.[19-22] As a result, it has thus been taken as a true signature of the O_3 PES and was incorporated into the hybrid O_3 PES developed by Babikov et al.,[17] as shown in Fig. A.1.

The asymptotic regions of the PES, in particular the ″reef″ feature, have important implications for kinetics. The cross section for the O + O_2 exchange reaction is dominated by large impact parameter collisions,[23] where the centrifugal potential transforms the ″reef″ into a real barrier at large *J* values. Two important consequences follow.[18,24] First, the calculated rate constants are about 3-5 times smaller than the measured ones. Second and perhaps more importantly, these calculated rate constants have qualitatively different temperature dependence from the experimental kinetic data,[25-27] which show a negative slope with *T*. The theory-experiment differences cannot be attributed to non-adiabatic interactions in the O + O_2 asymptote, as shown by Tashiro and Schinke.[28] So what could be the source of the discrepancies?
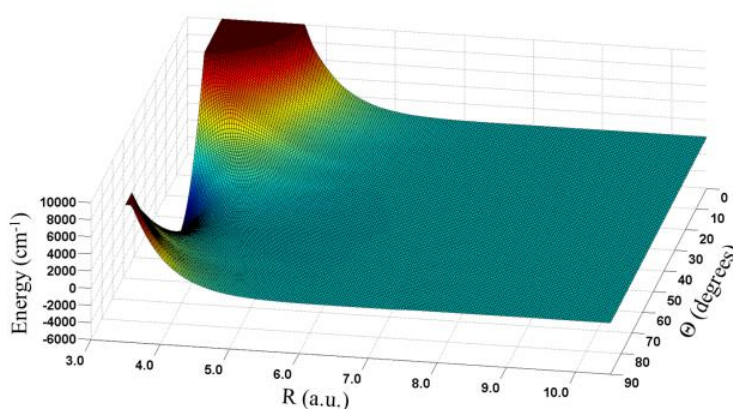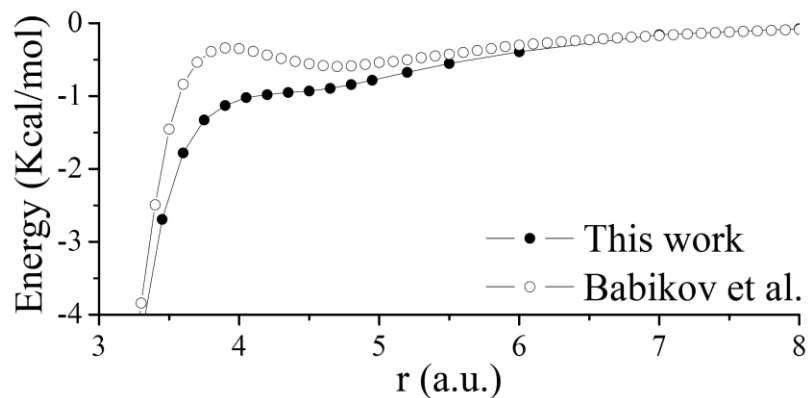
Figure A.1 Upper panel: minimal energy path for O_3 formation along an O-O bond length obtained in this work (filled circles) and its comparison with that on the hybrid PES of Babikov et al.[17] (open circles). Lower panel: the corresponding two-dimensional potential energy surface in the $O-O_2$ Jacobi coordinates.

A hypothetic numerical ″experiment″ performed by Schinke and coworkers is quite revealing.[18] These authors found that the artificial removal of the ″reef″ structure in the O_3 PES substantially increased the reaction cross section and brought the calculated rate constants to good agreement with experiment. Nonetheless, this modification of the O_3 PES was dismissed for lack of support from electronic structure theory.

To resolve this puzzle, we have undertaken extensive *ab initio* calculations at the MRCI level[29-30] with Davidson correction,[31] using MOLPRO.[32] Considering adiabatic dissociation of ozone in the C_s group:

$$O_3(^1A') \rightarrow O(^3\Sigma_g^-) + O(^3P_g),$$
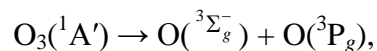
Σ_g^- corresponds to A'' and P_g corresponds to (A' + 2A''), combining to give (2A' + A''). Diabatically, the ground state of ozone correlates to excited states of both the atomic and molecular oxygen products:

$$O_3(^1A') \rightarrow O_2(^1\Delta_g) + O(^1D_g),$$
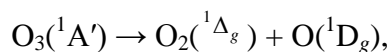
where Δ_g correlates to (A' + A''), and D_g correlates to (3A' + 2A''), combining to give (5A' + 5A''), a ten-fold asymptotic degeneracy of the excited states. Thus there are a total of 13 singlet states (7A', 6A'') potentially relevant to the dissociation of ozone.

Some of these states interact strongly in the transition region. Indeed, the "reef"-like structure observed in some calculations is due to an avoided crossing between the ground state in the molecular well (correlating diabatically with excited products) and the lowest-lying excited $^1A'$ state correlating with the $O_2(^3\Sigma_g^-) + O(^3P)$ asymptote.[16]

This raises the intriguing question of how many states should be included in calculating a global PES for ozone in its ground electronic state. In multistate CASSCF reference calculations, state averaging (SA) variationally optimizes the weighted-average energy of included states based on pre-assigned weights. If the ground state is well

separated from the excited state, such as the case of ozone near its equilibrium geometry, it is sufficient to include only the ground $^1A'$ state in CASSCF. While this strategy maximizes convergence of the ground state, it can lead to root flipping and other convergence problems toward the asymptote where multiple electronic states become quasi-degenerate. The MRCI studies of the asymptotic region by Schinke and coworkers[16] have thus included the three $(2A' + A'')$ asymptotically degenerate states (with equal weights) as a SA-CASSCF reference. However, the ″reef″ structure in the transition region is caused by an avoided crossing with a higher lying excited state, which was not included.

To explore the effect of including 13 singlet states in the CASSCF calculations, we have used the method of dynamical weighting.[33-34] With an energy-dependent weighting function, the DW-SA-CASSCF method typically includes many more states (than fixed weight calculations) without compromising convergence of the state of interest. At a given geometry the largest weight is assigned to the state of interest while weights for other states are assigned (self-consistently) based on their energy difference to the state of interest. Consequently, far-away states receive negligible weights, while neighboring states are heavily weighted. Furthermore, a far-away state that becomes closer in energy will see its weight increased, and *vice versa*. This allows the electronic wavefunction to smoothly evolve across the PES and correctly preserves differing asymptotic electronic state degeneracy patterns. For a given choice of included states there are typically crossings with still higher lying excluded states. The DW scheme allows those crossings

to occur seamlessly due to the negligible weights assigned to the states that are switching character.

We have carried out extensive MRCI calculations of the ozone formation potential with various basis sets and active spaces. These results are summarized in Supporting Information (SI). In Fig. A.1, we compare our newly calculated minimal energy path (MEP) for the formation of ozone with that on the hybrid PES of Babikov et al.[17] Contrary to previous studies, the MRCI calculations reported here used the two lowest full-valence 13-state DW-SA-CASSCF reference wavefunctions, instead of one such reference wavefunction. The results were extrapolated with AVTZ and AVQZ basis sets to the CBS limit. In addition, the rotated reference Davidson (+Q) correction was included. As shown in SI, the Davidson correction is relatively large in the results presented here, underscoring the importance of high order excitations for this system. The MEP was obtained by relaxing the O-O distance and O-O-O angle as the atomic oxygen approaches the molecular oxygen.

It is clear from Fig. A.1 that the new MEP is a monotonically decaying function of the dissociation coordinate. The disappearance of the ″reef″ structure is attributed primarily to including the ten upper states in the DW-SA-CASSCF reference, which smoothes the transition through the region of the avoided crossing. Also in the subsequent MRCI calculation a small, but significant mixing occurs between the ground and first excited A′ state (both are included in the MRCI calculations). Interestingly, if the ten upper states are excluded from the DW-SA-CASSCF reference and only one A′

state is included in the MRCI calculation, as shown in SI, our results indeed reproduce the "reef" structure.

We have constructed a two-dimensional PES at the same level of theory, using Jacobi coordinates with the O-O distance fixed at 2.2819 bohr. The PES, which was fitted using the IMLS method[35-36] with 120 points, is also shown in Fig. A.1. Using this PES, we have computed the thermal rate constant for the exchange reaction $^{16}O + {}^{32}O_2 \rightarrow {}^{32}O_2 + {}^{16}O$, using a quantum statistical model (QSM).[24] While the computational details are given in SI, we note here that all odd O_2 rotational states up to $j=21$ were included and the partial waves were summed to $J_{max}=80$. In Fig. A.2, the calculated rate constant is compared with available experimental data and previous theoretical data. It is clear that the absence of the "reef" structure in the PES produces a substantial enhancement of the rate constant, bringing it into much better agreement with experimental data. More importantly, the calculated rate is now in qualitative agreement with the experiment in the negative temperature dependence, a signature of barrierless reactions. We note here that the QSM model is an approximation, as the exchange reaction is known to have a strong non-statistical component.[23] While exact quantum dynamics calculations require a full-dimensional PES, the QSM results reported here strongly suggest that a new full-dimensional PES at this level of theory will close the gap between theory and experiment in this respect.

While the absence of the "reef" structure in the ozone formation potential has a large effect on kinetics, it is still not clear if it will significantly affect the reaction dynamics. It

is interesting to note that the minimal energy path has essentially the same O-O distance and O-O-O angle until it enters the deep O_3 well, as shown in SI. It is thus unlikely that dynamics for both the $O + O_2$ exchange and ozone formation reactions will be greatly affected. Indeed, using the PES of Babikov et al.,[17] reasonably good agreement with experiment has been found for product state distributions in the $O + O_2$ exchange reactions.[37] However, it is certainly worthwhile to revisit these issues when a full-dimensional PES using the same methods as reported here becomes available.
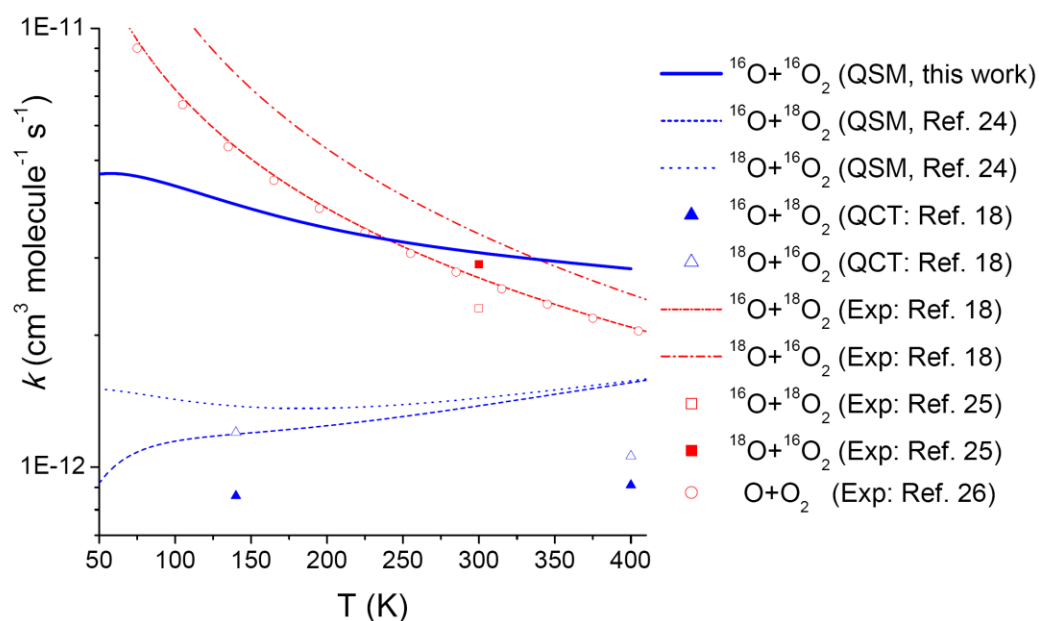
Figure A.2 Comparison of calculated (blue) and measured (red) rate constants for the $O + O_2$ exchange reactions. The quantum statistical model (QSM) and quasi-classical trajectory (QCT) results in Refs. 18 and 24 were obtained using the PES of Babikov et al.[17]

The dissociation energy of ozone has been another discrepancy between theory and experiment. Holka *et al.* reported recently a discrepancy of ~200 cm^{-1} between their best calculations and experiment.[22] The best current experimental estimate of D_0 for $O_3 \rightarrow O_2$

+ O is 8563.6 $\pm$ 3.5 cm^{-1}.[38] Accounting for the ZPEs of O_3 and O_2 results in an estimated D_e of 9234.1 cm^{-1} (there is more than 3.5 cm^{-1} uncertainty in D_e due to uncertainty in the ZPE of ozone). In Table A.1 dissociation energies are listed for various CBS extrapolation schemes (more detailed results are included in the SI). CBS energies are estimated using the l^{-3} formula as well as by separate extrapolation of the reference and correlation energies using a separately optimized power-law. Two implementations of the Davidson correction are compared, and a core-valence correlation correction (CV) was estimated from all-electron calculations. Scalar relativistic (SR) effects were computed and the effect of spin-orbit (SO) coupling was added.

Table A.1 Calculated MRCI dissociation energies (cm^{-1}) with applied relaxed (+Q_{rel}) or modified (+Q_{mod}) Davidson corrections.

Method		CBS34	CBS45	CBS56	CBS_pow
MRCI		8889.2	8792.3	8808.9	8765.7
MRCI(+Q_{rel})		9220	9114.5	9127	9079.8
MRCI(+Q_{mod})		9232.9	9127.4	9139.9	9093.2
Experiment		9234.1			

Including the smaller corrections (SO, CV and SR), D_e is certainly underestimated without Davidson corrections even at the CBS level. With Davidson corrections and various CBS extrapolations, calculated values for D_e vary by about 150 cm^{-1}, with the largest calculated value coming within experimental error. Near exact agreement comes from the simple l^{-3} extrapolation of the smaller triple and quadruple zeta bases, whereas CBS extrapolations of the largest bases with the l^{-3} formula or separate power-law extrapolation of the correlation energy produces values for D_e that are further from experiment. From these results it appears that D_e is quite well captured but the largest

remaining uncertainty lies in the CBS extrapolations. The significance of Davidson corrections also confirms the importance of higher-order correlation effects.

To summarize, we have shown in this work that dynamically weighted Davidson corrected multi-state multi-reference configuration intersection calculations allow a much more accurate characterization of the ozone formation potential. Specifically, the iconic ″reef″ structure in the minimal energy path is shown to be absent, due apparently to a smoother transition through the region of avoided crossing with a higher electronic state. The absence of this submerged barrier has important implications for kinetics. As we have demonstrated with an approximate quantum model, the new PES brings the calculated rate constant into much better agreement with experiment and produces a negative temperature dependence as observed experimentally. These new developments set the stage for future quantitative characterization of the $O + O_2$ exchange reaction and the ozone formation, including the understanding of the puzzling mass-independent fractionation phenomenon.

Supporting Information Available: Details of *ab initio* calculations and dynamic model, as well as additional results. This material is available free of charge via the Internet at http://pubs.acs.org

REFERENCES

[1]   Mauersberger, K. *Geophys. Res. Lett.* 1981, *8*, 935.

[2]   Thiemens, M. H.; Heidenreich III, J. E. *Science* 1983, *219*, 1073.

[3]   Weston, R. E. *Chem. Rev* 1999, *99*, 2115.

[4]   Mauersberger, K.; Krankowsky, D.; Janssen, C.; Schinke, R. *Adv. At. Mole. Opt. Phys.* 2005, *50*, 1.

[5]   Thiemens, M. H. *Annu. Rev. Earth Planet. Sci.* 2006, *34*, 217.

[6]   Janssen, C.; Guenther, J.; Mauersberger, K.; Krankowski, D. *Phys. Chem. Chem. Phys.* 2001, *3*, 4718.

[7]   Gao, Y. Q.; Marcus, R. A. *Science* 2001, *293*, 259.

[8]   Gao, Y. Q.; Marcus, R. A. *J. Chem. Phys.* 2002, *116*, 137.

[9]   Babikov, D.; Kendrick, B. K.; Walker, R. B.; Pack, R. T.; Fleurat-Lessard, P.; Schinke, R. *J. Chem. Phys.* 2003, *119*, 2577.

[10]   Schinke, R.; Fleurat-Lessard, P. *J. Chem. Phys.* 2005, *122*, 094317.

[11]   Xie, T.; Bowman, J. M. *Chem. Phys. Lett.* 2005, *412*, 131.

[12]   Grebenshchikov, S. Y.; Schinke, R. *J. Chem. Phys.* 2009, *131*, 181103.

[13]   Schinke, R.; Grebenshchikov, S. Y.; Ivanov, M. V.; Fleurat-Lessard, P. *Annu. Rev. Phys. Chem.* 2006, *57*, 625.

[14]   Muller, T.; Xantheas, S. S.; Dachsel, H.; Harrison, R. I.; Nieplocha, J.; Shepard, R.; Kedziora, G. S.; Lischka, H. *Chem. Phys. Lett.* 1998, *293*, 72.

[15]   Xie, D.; Guo, H.; Peterson, K. A. *J. Chem. Phys.* 2000, *112*, 8378.

[16]   Siebert, R.; Schinke, R.; Bittererova, M. *Phys. Chem. Chem. Phys.* 2001, *3*, 1795.

[17]   Babikov, D.; Kendrick, B. K.; Walker, R. B.; Pack, R. T.; Fleurat-Lesard, P.; Schinke, R. *J. Chem. Phys.* 2003, *118*, 6298.

[18]   Fleurat-Lessard, P.; Grebenshchikov, S. Y.; Siebert, R.; Schinke, R.; Halberstadt, N. *J. Chem. Phys.* 2003, *118*, 610.

[19]   Hernandez-Lamoneda, R.; Salazar, M. R.; Pack, R. T. *Chem. Phys. Lett.* 2002, *355*, 478.

[20]   Rosmus, P.; Palmieri, P.; Schinke, R. *J. Chem. Phys.* 2002, *117*, 4871.

[21]   Schinke, R.; Fleurat-Lessard, P. *J. Chem. Phys.* 2004, *121*, 5789.

[22]   Holka, F.; Szalay, P. G.; Muller, T.; Tyuterev, V. G. *J. Phys. Chem. A* 2010, *114*, 9927.

[23]   Sun, Z.; Liu, L.; Lin, S. Y.; Schinke, R.; Guo, H.; Zhang, D. H. *Proc. Nat. Acad. Sci.* 2010, *107*, 555.

[24]   Lin, S. Y.; Guo, H. *J. Phys. Chem. A* 2006, *110*, 5305.

[25]   Anderson, S. M.; Klein, F. S.; Kaufman, F. *J. Chem. Phys.* 1985, *83*, 1648.

[26]   Wiegell, M. R.; Larsen, N. W.; Pedersen, T.; Egsgaard, H. *Int. J. Chem. Kinet.* 1997, *29*, 745.

[27]   Fleurat-Lessard, P.; Grebenshchikov, S. Y.; Schinke, R.; Janssen, C.; Krankowsky, D. *J. Chem. Phys.* 2003, *119*, 4700.

[28]   Tashiro, M.; Schinke, R. *J. Chem. Phys.* 2003, *119*, 10186.

[29]   Knowles, P. J.; Werner, H.-J. *Chem. Phys. Lett.* 1988, *145*, 514.

[30]   Werner, H.-J.; Knowles, P. J. *J. Chem. Phys.* 1988, *89*, 5803.

[31]   Langhoff, S. R.; Davidson, E. R. *Int. J. Quant. Chem.* 1974, *8*, 61.

[32]   MOLPRO is a package of *ab initio* programs written by H.-J. Werner and P.J. Knowles with contributions from R. D. Amos et al.

[33]   Deskevich, M. P.; Nesbitt, D. J.; Werner, H.-J. *J. Chem. Phys.* 2004, *120*, 7281.

[34]   Dawes, R.; Jasper, A. W.; Tao, C.; Richmond, C.; Mukarakate, C.; Kable, S. H.; Reid, S. A. *J. Phys. Chem. Lett.* 2010, *1*, 641.

[35]   Dawes, R.; Thompson, D. L.; Wagner, A. F.; Minkoff, M. *J. Phys. Chem. A* 2009, *113*, 4709.

[36]   Dawes, R.; Wang, X.-G.; Jasper, A. W.; Carrington Jr., T. *J. Chem. Phys.* 2010, *134304* 133.

[37]   Van Wyngarden, A. L.; Mar, K. A.; Boering, K. A.; Lin, J. J.; Lee, Y. T.; Lin, S.-Y.; Guo, H.; Lendvay, G. *J. Am. Chem. Soc.* 2007, *129*, 2866.

[38]   Ruscic, B., private communication of ATcT result based on version 1.110 of the Core (Argonne) Thermochemical Network (May 17, 2010); B. Ruscic, R. E. Pinzon, M. L. Morton, G. von Laszewski, S. Bittner, S. G. Nijsure, K. A. Amin, M. Minkoff, and A. F. Wagner, J. Phys. Chem. A 108, 9979 (2004); B. Ruscic, R. E. Pinzon, G. von Laszewski, D. Kodeboyina, A. Burcat, D. Leahy, D. Montoya, and A. F. Wagner, J. Phys.: Conf. Ser. 16, 561 (2005); W. Klopper, B. Ruscic, D. P. Tew, F. A. Bischoff, and S. Wolfsegger, Chem. Phys. 356, 14 (2009).

APPENDIX B

LIST OF PUBLICATIONS

B. LIST OF PUBLICATIONS

[1] Richard Dawes, Phalgun Lolur, Jianyi Ma, and Hua Guo, "Communication: Highly accurate ozone formation potential and implications for kinetics". Published in *Journal of Chemical Physics.* 135, 081102 (2011). *http://dx.doi.org/10.1063/1.3632055*

[2] Chong Tao, Craig A. Richmond, Calvin Mukarakate, Scott H. Kable, George B. Bacskay, Eric C. Brown, Richard Dawes, Phalgun Lolur, and Scott A. Reid, "Spectroscopy and dynamics of the predissociated, quasi-linear S_2 state of chlorocarbene". Published in *Journal of Chemical Physics.* 137, 104307 (2012). *http://dx.doi.org/10.1063/1.4748972*

REFERENCES

[1] Mehra, J.; Rechenberg, H. (1982). The historical development of quantum theory.New York: Springer-Verlag. ISBN 0387906428.

[2] Celebrating Einstein "Solid Cold". U.S. DOE., Office of Scientific and Technical Information, 2011.

[3] Schrödinger, Erwin (December 1926). "An Undulatory Theory of the Mechanics of Atoms and Molecules". Phys. Rev. 28 (6) 28 (6): 1049–1070

[4] W. Heitler and F. London. Z. Physik 44, 455 (1927).

[5] D. R. Hartree. Proc. Cambridge Philos. Soc. 24, 328 (1928).

[6] V. A. Fock. Z. Phys. 15, 126 (1930).

[7] E. A. Hylleraas. Z. Physik 48, 469 (1928).

[8] C. Møller and M. S. Plesset. Phys. Rev. 46, 618 (1934).

[9] D. R. Hartree, W. Hartree, B. Swirles. Phil. Trans. Roy. Soc. (London) A238, 229 (1939).

[10] P. A. M. Dirac. Proc. Roy. Soc. (London) 123, 714 (1929).

[11] R. S. Mulliken and C. C. J. Roothaan, Proc. Natl. Acad. Sci. (U.S.) 45, 394 (1959).

[12] H. F. Schaefer. Quantum Chemistry: The Development of Ab Initio Methods in Molecular Electronic Structure Theory. Clarendon Press, Oxford (1984).

[13] M. Born and R. Oppenheimer. Zur Quantentheorie der Molekeln. Ann. Phys., 84:457, 1927.

[14] Frank Jensen. Introduction to Computational Chemistry. John Wiley and Sons, New York, 1999

[15] J. Simons. An Introduction to Theoretical Chemistry. Cambridge University Press, Cambridge, UK, 2003

[16] Levine, Ira N. (1991). Quantum Chemistry. Englewood Cliffs, New Jersey: Prentice Hall. pp. 455–544.

[17] Basis set - Davidson, Ernest; Feller, David (1986). "Basis set selection for molecular calculations". Chem. Rev. 86 (4)

[18] R. G. Parr and B. L. Crawford, Jr., J. Chem. Phys. 16, 526 (1948).

[19] A. J. Stone, The Theory of Intermolecular Forces, International Series of monographs on Chemistry, Vol. 32, (Clarendon Press, Oxford, 1996).

[20] G. C. Schatz, Reaction and Molecular Dynamics, Lecture Notes in Chemistry, Vol. 14, edited by A. Lagana and A. Riganelli (Springer, Berlin, 2000).

[21] D. L. Thompson and D. R. McLaughlin, Quasiclassical trajectory study of the H2 + F2 reactions. J. Chem. Phys. 62, 4284 (1975).

[22] N. Sathyamurthy, R. Rangarajan, and L. R. Raff, Reactive scattering on a spline-fitted ab initio surface: The He+H+2→HeH++H reaction. J. Chem. Phys. 64, 4606 (1976).

[23] J. M. Bowman, J. S. Bittman, and L. B. Harding, Ab initio calculations of the electronic and vibrational energies of HCO and HOC. J. Chem. Phys. 85, 911, (1986).

[24] B. G. Sumpter and D. W. Noid, Potential energy surfaces for macromolecules. A neural network technique. Chem. Phys. Lett. 192, 455 (1992).

[25] T. B. Blank, S. D. Brown, A. W. Calhoun, and D. J. Doren, Neural network models of potential energy surfaces. J. Chem. Phys. 103, 4129 (1994).

[26] J. Ischtwan and M. A. Collins, Molecular potential energy surfaces by interpolation. J. Chem. Phys. 100, 8080 (1994).

[27] M. J. T. Jordan, K. C. Thompson, and M. A. Collins, Convergence of molecular potential energy surfaces by interpolation: Application to the OH+H2→H2O+H reaction, J. Chem. Phys. 102, 5647 (1995).

[28] M. J. T. Jordan and M. A. Collins, An interpolated UHF potential energy surface for the OH+H2→H2O+H reaction. J. Chem. Phys. 104, 4600 (1996).

[29] D. F. R. Brown, M. N. Gibbs, and D. C. Clary, Combining ab initio computations, neural networks, and diffusion Monte Carlo: an efficient way to treat weakly bound molecules. J. Chem. Phys. 105, 7597 (1996).

[30] K. C. Thompson, M. J. T. Jordan, and M. A. Collins, Polyatomic molecular potential energy surfaces by interpolation in local internal coordinates. J. Chem. Phys. 108, 8302 (1998).

[31] V. Szalav, Iterative and direct methods employing distributed approximating functions for the reconstruction of a potential energy surface from its sampled values. J. Chem. Phys. 111, 8804 (1999).

[32] T. Ishida and G. C. Schatz, A local interpolation scheme using no derivatives in quantum chemical calculations. Chem. Phys. Lett. 314, 369 (1999).

[33] M. A. Collins, Molecular potential energy surfaces for chemical reaction dynamics. Theor. Chem. Acc. 108, 313 (2002).

[34] G. G. Maisuradze and D. L. Thompson, Interpolating moving least squares methods for fitting potential energy surfaces: Illustrative approaches and applications. J. Phys. Chem. A 107, 7118 (2003).

[35] G. G. Maisuradze, D. L. Thompson, A. F. Wagner, and M. Minkoff, Interpolating moving least squares methods for fitting potential energy surfaces: Detailed analysis of one-dimensional applications. J. Chem. Phys. 119, 10002 (2003).

[36] A. Kawano, Y. Guo, D. L. Thompson, A. F. Wagner, and M. Minkoff, Improving the accuracy of interpolated potential energy surfaces by using an analytical zeroth-order potential function. J. Chem. Phys. 120, 6414 (2004).

[37] Y. Guo, A. Kawano, D. L. Thompson, A. F. Wagner, and M. Minkoff, Interpolating moving least squares methods for fitting potential energy surfaces: applications to classical dynamics calculations. J. Chem. Phys. 121 (11), 5091 (2004).

[38] Y. Guo, L. B. Harding, A. F. Wagner, M. Minkoff, and D. L. Thompson, Interpolating moving least squares methods for fitting potential energy surfaces: an application to the H2CN unimolecular reaction. J. Chem. Phys. 126, 104105 (2007).

[39] R. Dawes, D. L. Thompson, Y. Guo, A. F. Wagner, and M. Minkoff, Interpolating moving least squares methods for fitting potential energy surfaces: computing high-density PES data from low-density ab initio points. J. Chem. Phys. 126, 184108 (2007).

[40] R. Dawes, D. L. Thompson, A. F. Wagner, and M. Minkoff, Interpolating moving least squares methods for fitting potential energy surfaces: a strategy for efficient automatic data point placement in high dimensions. J. Chem. Phys. 128, 84107 (2008).

[41] R. Dawes, A. Passalacqua, T. D. Sewell, A. F. Wagner, M. Minkoff, and D. L. Thompson Interpolating moving least squares methods for fitting potential energy surfaces: using classical trajectories to explore configuration space. J. Chem. Phys. 130, 144107 (2009).

[42] G. Czako, B. J. Braams, J. M. Bowman, Accurate ab initio structure, Dissociation energy and vibrational spectroscopy of the F--CH4 anion complex. J. Phys. Chem. A, 112, 7466 (2008).

[43] B. C. Shepler, B. J. Braams, J. M. Bowman, "Roaming" dynamics in CH3CHO photodissociation revealed on a global potential energy surface. J. Phys. Chem. A 112, 9344 (2008).

[44] Y. Wang, B. J. Braams, J. M. Bowman, S. Carter, D. P. Tew, Full-dimensional quantum calculations of ground-state tunneling splitting of malonaldehyde using an accurate potential energy surface. J. Chem. Phys. 128, 224314 (2008).

[45] Y. Wang, X. Huang, B. C. Shepler, B. J. Braams, and J. M. Bowman, Flexible, ab initio potential, and dipole moment surfaces for water. I. Tests and applications for clusters up to the 22-mer. J. Chem. Phys. 134, 94509 (2011).

[46] H. J. Werner, P. J. Knowles, R. Lindh, F. R. Manby, and M. Schultz, MOLPRO, a package of ab initio programs (2010)

[47] H.-J. Werner, P. J. Knowles, An efficient internally contracted MRCI method. J. Chem. Phys. 89, 5803 (1988).

[48] P. J. Knowles, H.-J. Werner, An efficient method for the evaluation of coupling coefficients in MRCI calculations. Chem. Phys. Lett. 145, 514 (1988).

[49] M. P. Deskevich, D. J. Nesbitt, H.-J. Werner, Dynamically weighted multiconfiguration self-consistent field: Multistate calculations for F+H2O→HF+OH reaction paths. J. Chem. Phys. 120, 7281 (2004).

[50] Brian Diffey. Climate change, ozone depletion and the impact on ultraviolet exposure of human skin. Phys. Med. Biol. 49 (2004).

[51] W Goettsch, J Garssen, W Slob, F R de Gruijl, H Van Loveren. Risk assessment for the harmful effects of UVB radiation on the immunological resistance to infectious diseases. Environ Health Perspect. 1998 February; 106(2): 71−77.

[52] Erica Harvey and Robert Sweeney, Modeling Stratospheric Ozone Kinetics, Part I. Journal of Chemical Education 1999, 76 (9), 1309.

[53] Erica Harvey and Robert Sweeney, Modeling Stratospheric Ozone Kinetics, Part II. Journal of Chemical Education 1999, 76 (9), 1310.

[54] P. Fleurat-Lessard, S. Y. Grebenshchikov, R. Siebert, R. Schinke, and N. Halberstadt, J. Chem. Phys. 118, 610 (2003).

[55] S. Y. Lin and H. Guo, J. Phys. Chem. A 110, 5305 (2006).

[56] S. M. Anderson, F. S. Klein, and F. Kaufman, J. Chem. Phys. 83, 1648(1985).

[57] M. R. Wiegell, N. W. Larsen, T. Pedersen, and H. Egsgaard, Int. J. Chem. Kinet. 29, 745 (1997).

[58] P. Fleurat-Lessard, S. Y. Grebenshchikov, R. Schinke, C. Janssen, and Krankowsky, J. Chem. Phys. 119, 4700 (2003).

[59] H.-J. Werner and P. J. Knowles, J. Chem. Phys. 89, 5803 (1988).

[60] P. J. Knowles and H.-J. Werner, Chem. Phys. Lett. 145, 514 (1988).

[61] S. R. Langhoff and E. R. Davidson, Int. J. Quant. Chem. 8, 61 (1974).

[62] T. H. Dunning, J. Chem. Phys. 90, 1007 (1989).

[63] Babikov, D.; Kendrick, B. K.; Walker, R. B.; Pack, R. T.; Fleurat-Lesard, P.; Schinke, R. J. Chem. Phys. 2003, 118, 6298.

VITA

Phalgun Lolur was born on July 9, 1989 in Adoni, India. He obtained his undergraduate degree in Chemical Engineering from Vellore Institute of Technology (VIT), Vellore, India in 2010. During his senior year, he interned at the Honeywell Technology Solutions Lab in Bangalore, India where he worked on Equipment Health Monitoring – Performance analysis of a Centrifugal Pump and a 1-2 Heat Exchanger. After his graduation, in Fall 2010 he started graduate studies in Chemical Engineering at Missouri University of Science and Technology, Rolla, Missouri.

During his course of study, he has worked on development of methods for computing and fitting global potential energy surfaces for molecular systems. He has published two papers (on ozone and CHCl) in the Journal of Chemical Physics (JCP), which are listed in the publications page. Apart from his research, Phalgun has held several executive positions in student organizations. He was the Vice-President of the Council of Graduate Students for the year 2011-2012. He was the event coordinator and the student council representative for the International Students' Club and multimedia committee head for the India Association for the year 2010-2011. He is also part of the Internship and Co-Op Advisory Committee on campus. He received his M.S. degree in Chemical Engineering from Missouri University of Science and Technology in May, 2013.